

© 2009 IEEE. Personal use of this material is permitted. Permission from IEEE must be obtained for all other uses, in any current or future media, including reprinting/republishing this material for advertising or promotional purposes, creating new collective works, for resale or redistribution to servers or lists, or reuse of any copyrighted component of this work in other works.

Self-Optimizing Adaptive Vibration Controller

Maciej Niedźwiecki, *Member, IEEE* and Michał Meller, *Student member, IEEE*

Abstract—This paper presents a new approach to rejection of sinusoidal disturbances acting at the output of a discrete-time linear stable plant with unknown dynamics. It is assumed that the frequency of the sinusoidal disturbance is known, and that the output signal is contaminated with wideband measurement noise. The proposed controller, called SONIC (Self-Optimizing Narrowband noise Canceller), combines the coefficient fixing technique, used to “robustify” self-tuning minimum-variance regulators, with automatic adaptation gain tuning. Both theoretical analysis and computer simulations confirm that, under Gaussian assumptions, the closed-loop system converges (locally) in mean to the optimal solution.

Index Terms—Adaptive control, disturbance rejection, system identification.

I. INTRODUCTION

CONSIDER the problem of cancellation of a narrowband disturbance $d(t)$, with known normalized (dimensionless) angular frequency $\omega_0 \in (0, \pi]$, corrupting the output of a discrete-time, stable linear plant of unknown dynamics, governed by

$$y(t) = K_0(q^{-1})u(t-1) + d(t) + v(t) \quad (1)$$

where $t = \dots, -1, 0, 1, \dots$ denotes normalized time, q^{-1} is the backward shift operator, $y(t)$ is the system output, $K_0(q^{-1})$ denotes unknown transfer function of the controlled plant, $u(t)$ is the system input, and $v(t)$ denotes a wideband measurement noise.

We will assume that the disturbance signal can be modeled as

$$d(t) = a_1(t) \sin \omega_0 t + a_2(t) \cos \omega_0 t = \boldsymbol{\alpha}^T(t) \mathbf{f}(t) \quad (2)$$

$$\boldsymbol{\alpha}(t) = [a_1(t), a_2(t)]^T, \quad \mathbf{f}(t) = [\sin \omega_0 t, \cos \omega_0 t]^T$$

where $a_1(t)$ and $a_2(t)$ denote slowly-varying weighting coefficients.

narrowband disturbances are usually generated by rotating elements of electro-mechanical systems and their elimination may be a very important control task, determining quality of the underlying technological processes such as turning, milling, grinding etc..

The problem of narrowband disturbance rejection was considered by many authors under different methodologies, such as internal model principle or the phase-locked loop based approach – see e.g. the recent work of Bodson and co-workers [1], [2], [3], [4], and Landau and co-workers [5], [6]. For an overview of different approaches see e.g. a tutorial paper [6].

An entirely new approach to cancellation of narrowband disturbances, based on coefficient fixing and automatic gain

The authors are with the Faculty of Electronics, Telecommunications and Computer Science, Department of Automatic Control, Gdańsk University of Technology, ul. Narutowicza 11/12, Gdańsk, Poland (e-mail: maciekn@eti.pg.gda.pl; michal.meller@eti.pg.gda.pl)

tuning, was proposed and analyzed in [7], [8]. The new method was developed for complex-valued systems, i.e., for systems where $y(t)$, $u(t)$, $d(t)$ and $v(t)$ are complex-valued signals. In particular, it was assumed that disturbance has the form

$$d(t) = a(t)e^{j\omega_0 t} \quad (3)$$

which can be considered a complex-valued counterpart of (2).

The main purpose of this paper is to extend the results presented in [7] to systems with real-valued input/output signals. This is a nontrivial task. We will show that for real-valued systems the analysis can be performed in a similar but not identical way as that carried for complex-valued systems. Such analysis requires different tools and leads to different quantitative results than those presented in [7]. Despite some obvious qualitative similarities, the disturbance canceling control algorithm for real-valued systems can't be obtained by transforming the analogous algorithm derived for complex-valued systems (and *vice versa*). This means that the investigation presented below is not a special case of the analysis carried in [7] – as a matter of fact the real-valued case is considerably more difficult to analyze than the complex-valued case.

The paper is organized as follows. Section II presents analysis of the open-loop disturbance rejection problem. The closed-loop problem is studied in Section III. The proposed self-optimizing disturbance rejection scheme, called SONIC (Self-Optimizing Narrowband noise Canceller), is presented in Section IV. Section V presents results of the mean convergence analysis of the closed-loop system and Section VI describes several safety measures that increase robustness of the adaptive regulator. Extensions to multiharmonic disturbances and to plants with an extra transport delay are discussed in Section VII. Section VIII shows the results of simulation experiments. Finally, Section IX concludes.

II. OPEN-LOOP CASE

Since the control loop incorporates a transport delay of one sampling interval, when shaping the input signal at instant t , one needs an accurate one-step-ahead prediction of $d(t+1)$, further denoted by $\hat{d}(t+1|t)$. Similarly as in the complex-valued case, we will base structure of the closed-loop predictor on the form of its open-loop analog.

Consider the problem of one-step-ahead prediction/compensation of a signal governed by

$$s(t) = d(t) + v(t) \quad (4)$$

where $d(t)$ is a harmonic disturbance, described by (2), and $v(t)$ denotes white measurement noise obeying

(A1) $\{v(t)\}$ is a sequence of uncorrelated, normally distributed random variables with zero mean and variance σ_v^2 : $v(t) \sim \mathcal{N}(0, \sigma_v^2)$.

To proceed further we will have to make some assumptions on the way the weighting coefficients $a_1(t)$ and $a_2(t)$, appearing in (2), vary with time. We will assume that both coefficients evolve, independently of each other, according to the random-walk (RW) model, namely¹

$$\boldsymbol{\alpha}(t) = \boldsymbol{\alpha}(t-1) + \mathbf{w}(t) \quad (5)$$

where

(A2) $\{\mathbf{w}(t)\}$, independent of $\{v(t)\}$, is a sequence of uncorrelated, normally distributed random variables with zero mean and covariance matrix $\mathbf{W} = \sigma_w^2 \mathbf{I}$: $\mathbf{w}(t) \sim \mathcal{N}(\mathbf{0}, \sigma_w^2 \mathbf{I})$.

and \mathbf{I} denotes a 2×2 identity matrix.

Even though pretty naïve from a practical viewpoint, such a model of variation will allow us to determine the lower bound on the mean-squared cancellation error, and hence to evaluate statistical efficiency of the proposed disturbance rejection scheme in absolute terms, rather than relative terms (e.g. by comparing it with one of the existing schemes).

Combining (2), (4) and (5), one arrives at the following state-space equations

$$\begin{aligned} \boldsymbol{\alpha}(t) &= \boldsymbol{\alpha}(t-1) + \mathbf{w}(t) \\ s(t) &= \boldsymbol{\alpha}^T(t) \mathbf{f}(t) + v(t). \end{aligned} \quad (6)$$

Denote by $\mathcal{S}(t) = \{s(1), \dots, s(t)\}$ the set of measurements available at instant t . The optimal, in the mean-square sense, one-step-ahead predictor of $s(t)$ has the form [9]

$$\hat{s}(t|t-1) = E[s(t)|\mathcal{S}(t-1)] = \hat{d}(t|t-1) = \hat{\boldsymbol{\alpha}}^T(t|t-1) \mathbf{f}(t)$$

where $\hat{\boldsymbol{\alpha}}(t|t-1) = E[\boldsymbol{\alpha}(t)|\mathcal{S}(t-1)]$ is a one-step-ahead predictor of $\boldsymbol{\alpha}(t)$. The mean-squared prediction error can be expressed in the form

$$E\{[s(t) - \hat{s}(t|t-1)]^2\} = E[c^2(t)] + \sigma_v^2$$

where $c(t) = d(t) - \hat{d}(t|t-1) = [\boldsymbol{\alpha}(t) - \hat{\boldsymbol{\alpha}}(t|t-1)]^T \mathbf{f}(t)$ will be further called cancellation error.

Under assumptions (A1) and (A2) the optimal estimates of $\boldsymbol{\alpha}(t)$ can be computed recursively using the celebrated Kalman filtering (KF) algorithm

$$\begin{aligned} \hat{\boldsymbol{\alpha}}(t|t) &= \hat{\boldsymbol{\alpha}}(t|t-1) + \mathbf{g}(t) \varepsilon(t) \\ \hat{\boldsymbol{\alpha}}(t|t-1) &= \hat{\boldsymbol{\alpha}}(t-1|t-1) \\ \varepsilon(t) &= s(t) - \hat{\boldsymbol{\alpha}}^T(t|t-1) \mathbf{f}(t) \\ \mathbf{g}(t) &= \frac{\mathbf{P}(t|t-1) \mathbf{f}(t)}{\sigma_v^2 + \mathbf{f}^T(t) \mathbf{P}(t|t-1) \mathbf{f}(t)} \\ \mathbf{P}(t|t-1) &= \mathbf{P}(t-1|t-1) + \sigma_w^2 \mathbf{I} \\ \mathbf{P}(t|t) &= \mathbf{P}(t|t-1) - \frac{\mathbf{P}(t|t-1) \mathbf{f}(t) \mathbf{f}^T(t) \mathbf{P}(t|t-1)}{\sigma_v^2 + \mathbf{f}^T(t) \mathbf{P}(t|t-1) \mathbf{f}(t)} \end{aligned} \quad (7)$$

where $\hat{\boldsymbol{\alpha}}(t|t) = E[\boldsymbol{\alpha}(t)|\mathcal{S}(t)]$ denotes the filtered estimate of $\boldsymbol{\alpha}(t)$, while $\mathbf{P}(t|t-1)$ and $\mathbf{P}(t|t)$ are the *a priori* and *a posteriori* error covariance matrices, respectively.

¹It is interesting to notice that when $\boldsymbol{\alpha}(t)$ obeys (5) the ratio $a_1(t)/a_2(t)$ slowly changes with time, which means that, strictly speaking, the instantaneous frequency of $d(t)$ is not constant but slowly varies around ω_0 .

Let $\xi = \sigma_w^2/\sigma_v^2$. When the vector $\boldsymbol{\alpha}(t)$ changes sufficiently slowly, namely when

$$\sqrt{\xi} = \frac{\sigma_w}{\sigma_v} \ll 1 \quad (8)$$

and when the “period” of $d(t)$, equal to $T_0 = 2\pi/\omega_0$, is sufficiently small (see Remark at the end of this section), the matrix $\mathbf{P}(t|t-1)$ is in steady state approximately constant

$$\begin{aligned} E_\infty\{[\boldsymbol{\alpha}(t) - \hat{\boldsymbol{\alpha}}(t|t-1)][\boldsymbol{\alpha}(t) - \hat{\boldsymbol{\alpha}}(t|t-1)]^T\} \\ = \lim_{t \rightarrow \infty} \mathbf{P}(t|t-1) \cong \mathbf{P}_\infty \end{aligned}$$

where E_∞ denotes the steady-state expectation: $E_\infty[x(t)] = \lim_{t \rightarrow \infty} E[x(t)]$ (whenever it exists). The limiting value of this matrix, denoted by \mathbf{P}_∞ , can be determined analytically using the deterministic averaging approach [10]. First, when condition (8) is fulfilled, it can be shown that for large values of t it holds that [11]

$$\mathbf{f}^T(t) \mathbf{P}(t|t-1) \mathbf{f}(t) \ll \sigma_v^2$$

leading to the following approximate relationship [cf. (7)]

$$\begin{aligned} \mathbf{P}(t+1|t) &\cong \mathbf{P}(t|t-1) \\ &\quad - \frac{1}{\sigma_v^2} \mathbf{P}(t|t-1) \mathbf{f}(t) \mathbf{f}^T(t) \mathbf{P}(t|t-1) + \sigma_w^2 \mathbf{I}. \end{aligned} \quad (9)$$

Second, since under the conditions specified above, variations in the covariance matrix $\mathbf{P}(t|t-1)$ are much slower than in the “regression” vector $\mathbf{f}(t)$, one can set

$$\mathbf{P}(t+1|t) \cong \mathbf{P}(t|t-1) \cong \dots \cong \mathbf{P}(t-T|t-T-1) \quad (10)$$

where T denotes the width of the local averaging window. Combining (9) with (10), one obtains

$$\mathbf{P}(t|t-1) \langle \mathbf{f}(t) \mathbf{f}^T(t) \rangle_T \mathbf{P}(t|t-1) \cong \sigma_v^2 \sigma_w^2 \mathbf{I} \quad (11)$$

where

$$\langle \mathbf{f}(t) \mathbf{f}^T(t) \rangle_T = \frac{1}{T} \sum_{i=t-T+1}^t \mathbf{f}(i) \mathbf{f}^T(i).$$

Note that

$$\lim_{T \rightarrow \infty} \langle \mathbf{f}(t) \mathbf{f}^T(t) \rangle_T = \langle \mathbf{f}(t) \mathbf{f}^T(t) \rangle_\infty = \frac{1}{2} \mathbf{I} \quad (12)$$

and that $\langle \mathbf{f}(t) \mathbf{f}^T(t) \rangle_T$ can be closely approximated by $\langle \mathbf{f}(t) \mathbf{f}^T(t) \rangle_\infty$ when $T \gg T_0$. This allows one to rewrite (11) in the form

$$\mathbf{P}(t|t-1) \mathbf{P}(t|t-1) \cong \mathbf{P}_\infty \mathbf{P}_\infty \cong 2 \sigma_v^2 \sigma_w^2 \mathbf{I}$$

leading to

$$\mathbf{P}_\infty \cong \sqrt{2} \sigma_v \sigma_w \mathbf{I}$$

and to the following steady-state recursive estimation formula

$$\hat{\boldsymbol{\alpha}}(t+1|t) = \hat{\boldsymbol{\alpha}}(t|t-1) + h_\infty \mathbf{f}(t) \varepsilon(t) \quad (13)$$

where $h_\infty = \sqrt{2} \sigma_w / \sigma_v = \sqrt{2\xi}$.

In an analogous way, assuming that the quantities $\boldsymbol{\alpha}(t)$ and $\hat{\boldsymbol{\alpha}}(t|t-1)$ change slowly compared to $\mathbf{f}(t)$, one can compute

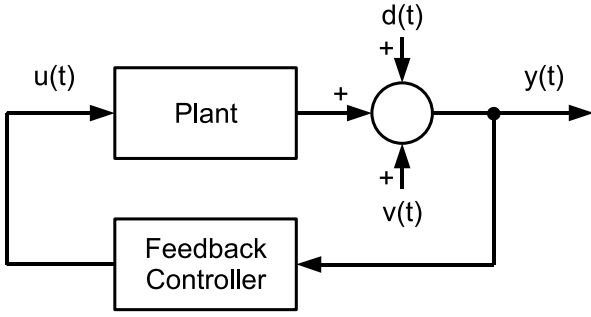


Fig. 1. Block diagram of the disturbance rejection system.

the steady-state mean-squared cancellation error yielded by the KF algorithm

$$\begin{aligned} E_{\infty}[\langle c^2(t) \rangle_{\infty}] &\cong \text{tr}\{\mathbf{P}_{\infty} \langle \mathbf{f}(t)\mathbf{f}^T(t) \rangle_{\infty}\} \\ &= \frac{1}{2} \text{tr}\{\mathbf{P}_{\infty}\} = \sqrt{2} \sigma_v \sigma_w. \end{aligned} \quad (14)$$

Since Kalman filter is the optimal estimation algorithm, the right-hand side of (14) determines the lowest achievable value of the mean-squared cancellation error for the problem at hand, sometimes referred to as the Bayesian Cramér-Rao bound [12] (the classical Cramér-Rao bound does not apply to systems/signals with random parameters).

Remark: For small values of ξ the time T over which the covariance matrix $\mathbf{P}(t|t-1)$ can be considered constant [cf. (10)] roughly corresponds to the equivalent estimation memory of the KF algorithm which, in the case considered, can be expressed in the form (see [13], Ch. 7 for more details)

$$l_{\infty} = \frac{2\sqrt{2}}{\sqrt{\xi}}.$$

Requiring that $T = l_{\infty} \gg T_0$, one arrives at the conditions

$$T_0 \ll \sqrt{\frac{8}{\xi}}, \quad \omega_0 \gg \pi\sqrt{\frac{\xi}{2}} \quad (15)$$

that must be fulfilled for our asymptotic analysis, based on averaging, to be valid.

Note that $\omega_0 = 2\pi f_0/f_s \in (0, \pi]$, where f_0 is the frequency (measured in Hertz) of the real-world, continuous-time disturbance and f_s denotes sampling frequency. Hence, the condition (15) can be always enforced by choosing an appropriately small sampling rate. When this is not feasible – by decreasing sampling frequency, one increases latency of the resulting discrete-time control system – one can treat disturbance $d(t)$, that does not fulfill (15), as a slowly-varying aperiodic signal: $d(t) = a(t)$, where $a(t)$ evolves according to the random-walk model. The algorithm (7) can still be used to compensate $d(t)$, provided that the quantities $\alpha(t)$ and $\mathbf{f}(t)$ (this time both scalar) are set to $a(t)$ and 1, respectively.

III. ADAPTIVE FEEDBACK CONTROLLER

We will look for the control signal that minimizes the mean-squared cancellation error for the system described by (1) – see Fig. 1. We will assume that the controlled plant is stable and has nonzero gain at frequency ω_0 :

$$(A3) \quad K_0(q^{-1}) = \sum_{i=0}^{\infty} f_i q^{-i}, \quad \sum_{i=0}^{\infty} |f_i| < \infty, \\ K_0(e^{-j\omega_0}) \neq 0$$

but we will *not* assume that its transfer function $K_0(q^{-1})$ is known.

A. Adaptive control rule

Vaguely speaking, to cancel sinusoidal disturbance $d(t)$, one should generate such sinusoidal input signal $u(t)$ which, after passing through the plant, will have the same shape as $d(t)$ but opposite polarity. Note that the steady-state response of a linear system to the sinusoidal input signal $u(t) = \alpha^T \mathbf{f}(t)$ can be written in the form

$$K_0(q^{-1})\alpha^T \mathbf{f}(t) = \alpha^T \mathbf{K}_0 \mathbf{f}(t) \quad (16)$$

where

$$\begin{aligned} \mathbf{K}_0 &= \begin{bmatrix} \text{Re}\{K_0(e^{-j\omega_0})\} & \text{Im}\{K_0(e^{-j\omega_0})\} \\ -\text{Im}\{K_0(e^{-j\omega_0})\} & \text{Re}\{K_0(e^{-j\omega_0})\} \end{bmatrix} \\ &= k_0 \begin{bmatrix} \cos \phi_0 & \sin \phi_0 \\ -\sin \phi_0 & \cos \phi_0 \end{bmatrix}. \end{aligned}$$

The quantities $k_0 = |K_0(e^{-j\omega_0})|$ and $\phi_0 = \arg[K_0(e^{-j\omega_0})]$ can be recognized as a true plant gain at frequency ω_0 and its true phase shift, respectively.

Therefore, had the matrix \mathbf{K}_0 been known, the following disturbance rejection rule could have been used

$$u(t) = -\hat{\alpha}^T(t+1|t)\mathbf{K}_0^{-1}\mathbf{f}(t+1).$$

According to (16), for such control signal the cancellation error can be approximately expressed in the form²

$$\begin{aligned} c(t) &= K_0(q^{-1})u(t-1) + d(t) \\ &\cong d(t) - \hat{\alpha}^T(t|t-1)\mathbf{K}_0^{-1}\mathbf{K}_0\mathbf{f}(t) \\ &= d(t) - \hat{\alpha}^T(t|t-1)\mathbf{f}(t) = [\alpha(t) - \hat{\alpha}(t|t-1)]^T \mathbf{f}(t) \end{aligned}$$

which is identical with an analogous expression derived in the open-loop case. Since the transfer function $K_0(q^{-1})$ is unknown, the actual control rule will have the form

$$u(t) = -\hat{\alpha}^T(t+1|t)\mathbf{K}_n^{-1}\mathbf{f}(t+1) \quad (17)$$

where

$$\begin{aligned} \mathbf{K}_n &= \begin{bmatrix} \text{Re}\{K_n(e^{-j\omega_0})\} & \text{Im}\{K_n(e^{-j\omega_0})\} \\ -\text{Im}\{K_n(e^{-j\omega_0})\} & \text{Re}\{K_n(e^{-j\omega_0})\} \end{bmatrix} \\ &= k_n \begin{bmatrix} \cos \phi_n & \sin \phi_n \\ -\sin \phi_n & \cos \phi_n \end{bmatrix} \\ k_n &= |K_n(e^{-j\omega_0})|, \quad \phi_n = \arg[K_n(e^{-j\omega_0})] \end{aligned}$$

and $K_n(q^{-1})$ denotes the nominal (assumed) transfer function of the plant. Similarly as in [7], we will design the one-step-ahead predictor $\hat{d}(t+1|t) = \hat{\alpha}^T(t+1|t)\mathbf{f}(t+1)$ in such a way that will guarantee automatic compensation of modeling errors. For this reason the nominal gain k_n and nominal phase ϕ_n will be considered nothing more than a convenient starting point for the adaptive control algorithm.

²For some further comments on this approximation see Remark 2 at the end of this section

Under (17) the output of the system can be approximately written down in the form

$$y(t) \cong c(t) + v(t) \quad (18)$$

where

$$c(t) = [\boldsymbol{\alpha}(t) - \mathbf{B}^T \hat{\boldsymbol{\alpha}}(t|t-1)]^T \mathbf{f}(t)$$

and

$$\mathbf{B} = \mathbf{K}_n^{-1} \mathbf{K}_0 = \begin{bmatrix} \operatorname{Re}\{\beta\} & \operatorname{Im}\{\beta\} \\ -\operatorname{Im}\{\beta\} & \operatorname{Re}\{\beta\} \end{bmatrix}, \quad \beta = \frac{K_0(e^{-j\omega_0})}{K_n(e^{-j\omega_0})}.$$

Note that the quantity $|\beta| = k_0/k_n$ is the gain modeling error, and the quantity $\arg\beta = \phi_0 - \phi_n = \Delta\phi$ constitutes the phase error.

The one-step-ahead predictor of $\boldsymbol{\alpha}(t)$ will be computed recursively using

$$\hat{\boldsymbol{\alpha}}(t+1|t) = \hat{\boldsymbol{\alpha}}(t|t-1) + \mathbf{M}\mathbf{f}(t)y(t) \quad (19)$$

where

$$\mathbf{M} = \begin{bmatrix} \operatorname{Re}\{\mu\} & -\operatorname{Im}\{\mu\} \\ \operatorname{Im}\{\mu\} & \operatorname{Re}\{\mu\} \end{bmatrix}$$

and μ denotes a complex-valued adaptation gain. For the real-valued adaptation gain ($\operatorname{Im}\{\mu\} = 0$) the second term on the right-hand side of (19) takes the form $\mu\mathbf{f}(t)y(t)$ and resembles the analogous term in (13). Later on we will show that application of a complex-valued gain is crucial as it allows one to compensate phase errors.

B. Tracking analysis

Substituting the right-hand side of (18) into (19), one obtains

$$\hat{\boldsymbol{\alpha}}(t+1|t) = \hat{\boldsymbol{\alpha}}(t|t-1) + \mathbf{M}\mathbf{f}(t)\mathbf{f}^T(t)[\boldsymbol{\alpha}(t) - \mathbf{B}^T \hat{\boldsymbol{\alpha}}(t|t-1)] + \mathbf{M}\mathbf{f}(t)v(t). \quad (20)$$

Let

$$\Delta\hat{\boldsymbol{\alpha}}(t) = \boldsymbol{\alpha}(t) - \mathbf{B}^T \hat{\boldsymbol{\alpha}}(t|t-1).$$

Combining (5) and (20), one arrives at

$$\begin{aligned} \Delta\hat{\boldsymbol{\alpha}}(t+1) &= (\mathbf{I} - \mathbf{B}^T \mathbf{M}\mathbf{f}(t)\mathbf{f}^T(t))\Delta\hat{\boldsymbol{\alpha}}(t) \\ &\quad - \mathbf{B}^T \mathbf{M}\mathbf{f}(t)v(t) + \mathbf{w}(t+1) \\ &\cong (\mathbf{I} - \mathbf{B}^T \mathbf{M}/2)\Delta\hat{\boldsymbol{\alpha}}(t) - \mathbf{B}^T \mathbf{M}\mathbf{f}(t)v(t) + \mathbf{w}(t+1) \end{aligned} \quad (21)$$

where, similarly to Section II, the approximation stems from the averaging theory. This leads to

$$E[\Delta\hat{\boldsymbol{\alpha}}(t+1)] = (\mathbf{I} - \mathbf{B}^T \mathbf{M}/2)E[\Delta\hat{\boldsymbol{\alpha}}(t)]. \quad (22)$$

Note that the matrix $\mathbf{B}^T \mathbf{M}$ can be expressed in the form

$$\mathbf{B}^T \mathbf{M} = \begin{bmatrix} \operatorname{Re}\{\beta\mu\} & -\operatorname{Im}\{\beta\mu\} \\ \operatorname{Im}\{\beta\mu\} & \operatorname{Re}\{\beta\mu\} \end{bmatrix}.$$

When $\mu \in \Omega_s$, where

$$\Omega_s = \left\{ \mu : \left(1 - \frac{\operatorname{Re}\{\beta\mu\}}{2}\right)^2 + \left(\frac{\operatorname{Im}\{\beta\mu\}}{2}\right)^2 < 1 \right\} \quad (23)$$

both eigenvalues of the matrix $\mathbf{I} - \mathbf{B}^T \mathbf{M}/2$ lie inside the unit circle in complex plane, leading to

$$E[\Delta\hat{\boldsymbol{\alpha}}(t)] \xrightarrow{t \rightarrow \infty} 0$$

which entails $E_\infty[c(t)] = 0$. This means that when μ lies in the stability area Ω_s , the steady-state mean value of the cancellation error is zero even if $\beta \neq 1$, i.e., even if the assumed values of the gain and phase shift differ from the true values.

We will derive expression for the mean-squared cancelling error. Observe that

$$\begin{aligned} E_\infty[\langle c^2(t) \rangle_\infty] &= E_\infty[\Delta\hat{\boldsymbol{\alpha}}^T(t) \langle \mathbf{f}(t)\mathbf{f}^T(t) \rangle_\infty \Delta\hat{\boldsymbol{\alpha}}(t)] \\ &= E_\infty[\|\Delta\hat{\boldsymbol{\alpha}}(t)\|^2]/2. \end{aligned} \quad (24)$$

Due to mutual orthogonality of $\Delta\hat{\boldsymbol{\alpha}}(t)$, $v(t)$ and $\mathbf{w}(t+1)$, after squaring both sides of (21) and taking expectations, one obtains

$$\begin{aligned} E[\|\Delta\hat{\boldsymbol{\alpha}}(t+1)\|^2] &= E[\Delta\hat{\boldsymbol{\alpha}}^T(t)(\mathbf{I} - \mathbf{f}(t)\mathbf{f}^T(t)\mathbf{M}^T\mathbf{B}) \times \\ &\quad \times (\mathbf{I} - \mathbf{B}^T \mathbf{M}\mathbf{f}(t)\mathbf{f}^T(t))\Delta\hat{\boldsymbol{\alpha}}(t) \\ &\quad + \mathbf{f}^T(t)\mathbf{M}^T \mathbf{B}\mathbf{B}^T \mathbf{M}\mathbf{f}(t)E[v^2(t)] + E[\|\mathbf{w}(t+1)\|^2]]. \end{aligned} \quad (25)$$

Since $\mathbf{B}\mathbf{B}^T = |\beta|^2 \mathbf{I}$, $\mathbf{M}\mathbf{M}^T = |\mu|^2 \mathbf{I}$, $\mathbf{f}^T(t)\mathbf{f}(t) \equiv 1$ and $\mathbf{M}^T \mathbf{B} + \mathbf{B}^T \mathbf{M} = (\beta\mu + \beta^* \mu^*) \mathbf{I} = 2\operatorname{Re}[\beta\mu] \mathbf{I}$, where $*$ denotes complex conjugation, one obtains

$$\begin{aligned} \mathbf{f}^T(t)\mathbf{M}^T \mathbf{B}\mathbf{B}^T \mathbf{M}\mathbf{f}(t) &= |\beta\mu|^2 \\ \boldsymbol{\Sigma}(t) &= (\mathbf{I} - \mathbf{f}(t)\mathbf{f}^T(t)\mathbf{M}^T \mathbf{B})(\mathbf{I} - \mathbf{B}^T \mathbf{M}\mathbf{f}(t)\mathbf{f}^T(t)) \\ &= \mathbf{I} - \mathbf{f}(t)\mathbf{f}^T(t)\mathbf{M}^T \mathbf{B} - \mathbf{B}^T \mathbf{M}\mathbf{f}(t)\mathbf{f}^T(t) \\ &\quad + |\beta\mu|^2 \mathbf{f}(t)\mathbf{f}^T(t) \end{aligned}$$

and, using averaging

$$\begin{aligned} E[\Delta\hat{\boldsymbol{\alpha}}^T(t)\boldsymbol{\Sigma}(t)\Delta\hat{\boldsymbol{\alpha}}(t)] &\cong E[\Delta\hat{\boldsymbol{\alpha}}^T(t) \langle \boldsymbol{\Sigma}(t) \rangle_\infty \Delta\hat{\boldsymbol{\alpha}}(t)] \\ &\cong \{1 - \operatorname{Re}[\beta\mu] + |\beta\mu|^2/2\} E[\|\Delta\hat{\boldsymbol{\alpha}}(t)\|^2]. \end{aligned}$$

This leads to the following steady-state relationship

$$\begin{aligned} E_\infty[\|\Delta\hat{\boldsymbol{\alpha}}(t)\|^2] &= \{1 - \operatorname{Re}[\beta\mu] + |\beta\mu|^2/2\} E_\infty[\|\Delta\hat{\boldsymbol{\alpha}}(t)\|^2] \\ &\quad + |\beta\mu|^2 \sigma_v^2 + 2\sigma_w^2. \end{aligned}$$

Finally, solving the above equation with respect to $E_\infty[\|\Delta\hat{\boldsymbol{\alpha}}(t)\|^2]$, one arrives at [cf. (24)]

$$\begin{aligned} E_\infty[\langle c^2(t) \rangle_\infty] &= E_\infty[\|\Delta\hat{\boldsymbol{\alpha}}(t)\|^2]/2 \\ &= \frac{\sigma_w^2 + |\beta\mu|^2 \sigma_v^2/2}{\operatorname{Re}[\beta\mu] - |\beta\mu|^2/2}. \end{aligned} \quad (26)$$

Denote by μ_{opt} the gain that minimizes the mean-squared cancellation error. Straightforward calculations lead to

$$\mu_{\text{opt}} = \arg \min_{\mu \in \Omega_s} E_\infty[\langle c^2(t) \rangle_\infty] = \frac{1}{\beta} \left[-\xi + \sqrt{\xi^2 + 2\xi} \right]. \quad (27)$$

When the slow variation condition (8) is fulfilled, one obtains $\mu_{\text{opt}} \cong \sqrt{2\xi}/\beta = h_\infty/\beta$ and

$$E_\infty[\langle c^2(t) \rangle_\infty | \mu = \mu_{\text{opt}}] \cong \sqrt{2} \sigma_v \sigma_w. \quad (28)$$

Note that the right-hand side of (28) coincides with the right-hand side of (14). This means that, no matter how large the gain and phase mismatch, one can always choose such value of the adaptation gain μ that will make the disturbance rejection scheme statistically efficient. In next section we will propose a method for automatic adjustment of the adaptation gain μ .

Remark 1: Suppose that, analogously as in the Kalman filter algorithm (13), a scalar, real-valued gain $\mu > 0$ is used in (19) instead of the matrix gain \mathbf{M} , i.e., that $\mathbf{M} = \mu\mathbf{I}$. Then, under (8), it holds that

$$\mu'_{\text{opt}} = \arg \min_{\mu \in \mathbb{R}_+} E_{\infty}[\langle c^2(t) \rangle_{\infty}] \cong \sqrt{2\xi} / |\beta|$$

and

$$E_{\infty}[\langle c^2(t) \rangle_{\infty} | \mu = \mu'_{\text{opt}}] \cong \frac{\sqrt{2} \sigma_v \sigma_w}{\cos \Delta\phi} \quad (29)$$

where $\Delta\phi = \arg\beta$, which means that even if μ is chosen in the optimal way, for large phase errors one may face substantial losses in rejection efficiency. Application of a matrix gain is therefore a *necessary* condition for compensation of phase modeling errors. It allows one to avoid performance degradation.

Remark 2: When deriving the expression (26), describing dependence of the mean-squared cancellation error on μ , we have exploited the steady-state approximation (16), stemming from the fact that linear systems basically scale and shift in phase sinusoidal inputs. Another source of approximation errors is due to averaging. A special simulation experiment was arranged to check how well the resulting theoretical formula fits the true error values. The simulated discrete-time plant

$$K_0(z) = 0.0952 / (1 - 0.9048z^{-1}) \quad (30)$$

was adopted from [4] and corresponds to a continuous-time plant with transfer function $P(s) = 1 / (1 + 0.01s)$ sampled at the rate of 1 kHz. Simulations were carried for $\sigma_v = 0.1$ and for 4 different rates of amplitude variation $\sigma_w \in \{0.0001, 0.0005, 0.001, 0.005\}$, in the absence of modeling errors ($\beta = 1$). For each (σ_w, μ) pair the experiment, covering 20000 time-steps, was repeated 500 times for different realizations of $\{v(t)\}$ and $\{w(t)\}$. In all cases $\alpha(0)$ was set to $[1, 1]^T$ and $\hat{\alpha}(0)$ was set to $[0, 0]^T$.

The results, summarized in Fig. 2, were obtained by means of combined ensemble and time averaging, after discarding the first 10000 samples (to ensure that the steady-state conditions are reached). Note the good agreement of experimental values with theoretical expectations for the considered (and practically meaningful) range of adaptation gains.

IV. SELF-OPTIMIZING CONTROLLER

In this section we will design an adaptive algorithm for on-line tuning of a complex-valued adaptation gain μ . We will adjust μ recursively by minimizing the following local measure of fit, made up of exponentially weighted system outputs

$$V(t; \mu) = \frac{1}{2} \sum_{i=1}^t \rho^{t-i} y^2(i; \mu).$$

The forgetting constant ρ ($0 < \rho < 1$) determines the effective averaging range. To evaluate the estimate $\hat{\mu}(t) = \arg \min_{\mu \in \mathbb{C}} V(t; \mu)$ we will use the recursive prediction error (RPE) approach [14]

$$\hat{\mu}(t) = \hat{\mu}(t-1) - [V''(t; \hat{\mu}(t-1))]^{-1} V'(t; \hat{\mu}(t-1))$$

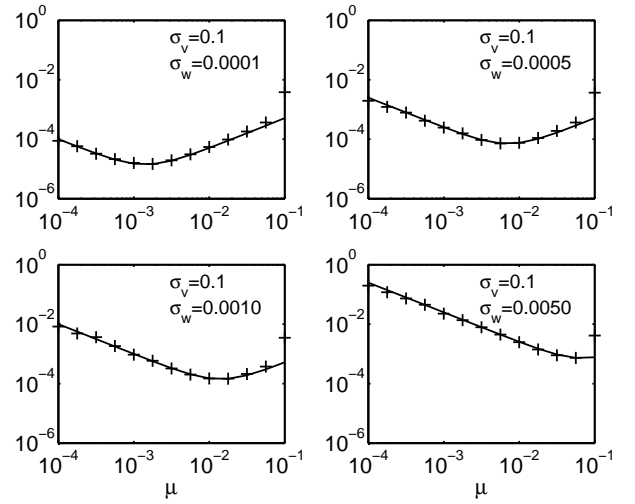


Fig. 2. Comparison of theoretical values of the mean-squared cancellation error, obtained using the steady-state plant approximation (solid line), with the experimental values (crosses).

where

$$V'(t; \hat{\mu}(t-1)) \cong \left(\frac{\partial y(t; \hat{\mu}(t-1))}{\partial \mu} \right)^* y(t; \hat{\mu}(t-1))$$

$$V''(t; \hat{\mu}(t-1)) \cong \rho V''(t-1; \hat{\mu}(t-2)) + \left| \frac{\partial y(t; \hat{\mu}(t-1))}{\partial \mu} \right|^2$$

and the operator of symbolic differentiation with respect to a complex variable, known also as Wirtinger derivative, is defined as [15]

$$\frac{\partial}{\partial \mu} = \frac{1}{2} \left[\frac{\partial}{\partial \text{Re}[\mu]} - j \frac{\partial}{\partial \text{Im}[\mu]} \right].$$

Using Wirtinger calculus, one obtains

$$\frac{\partial y(t)}{\partial \mu} = -\mathbf{f}^T(t) \mathbf{B}^T \frac{\partial \hat{\alpha}(t|t-1)}{\partial \mu}$$

$$\frac{\partial \hat{\alpha}(t+1|t)}{\partial \mu} = \frac{\partial \hat{\alpha}(t|t-1)}{\partial \mu} + \mathbf{M} \mathbf{f}(t) \frac{\partial y(t)}{\partial \mu} + \frac{\partial \mathbf{M}}{\partial \mu} \mathbf{f}(t) y(t). \quad (31)$$

Note that

$$\frac{\partial \mathbf{M}}{\partial \mu} = \frac{1}{2} \begin{bmatrix} 1 & j \\ -j & 1 \end{bmatrix} = \mathbf{H}. \quad (32)$$

Since the matrix \mathbf{B} is not known, the obtained recursive formulas can't be used in their present form. To circumvent this problem we will use the coefficient fixing technique introduced in [7], namely we will set $\beta = c_{\mu} / \mu$, where c_{μ} denotes a small positive constant. This leads to³

$$\mathbf{B}^T = c_{\mu} \mathbf{M}^{-1} \quad (33)$$

³According to (27), for the optimal choice of μ the matrix gain $\mathbf{M} \mathbf{B}^T = \mathbf{B} \mathbf{M}^T$, determining properties of the closed-loop system, reduces to $h_{\infty} \mathbf{I}$. Note that (33), which entails $\mathbf{M} \mathbf{B}^T = c_{\mu} \mathbf{I}$, preserves structure of the optimal solution.

and results in the following modified recursions

$$\begin{aligned}\frac{\partial y(t)}{\partial \mu} &= -c_\mu \mathbf{f}^\top(t) \mathbf{M}^{-1} \frac{\partial \hat{\alpha}(t|t-1)}{\partial \mu} \\ \frac{\partial \hat{\alpha}(t+1|t)}{\partial \mu} &= \frac{\partial \hat{\alpha}(t|t-1)}{\partial \mu} + \mathbf{M} \mathbf{f}(t) \frac{\partial y(t)}{\partial \mu} \\ &\quad + \mathbf{H} \mathbf{f}(t) y(t).\end{aligned}\quad (34)$$

Using averaging the second recursion in (34) can be rewritten in the following approximate form

$$\begin{aligned}\frac{\partial \hat{\alpha}(t+1|t)}{\partial \mu} &= (\mathbf{I} - c_\mu \mathbf{M} \mathbf{f}(t) \mathbf{f}^\top(t) \mathbf{M}^{-1}) \frac{\partial \hat{\alpha}(t|t-1)}{\partial \mu} \\ &\quad + \mathbf{H} \mathbf{f}(t) y(t) \\ &\cong (1 - |\mu|/2) \frac{\partial \hat{\alpha}(t|t-1)}{\partial \mu} + \mathbf{H} \mathbf{f}(t) y(t)\end{aligned}$$

Hence, to guarantee stable operation of (34), one must request that $|1 - c_\mu/2| < 1$ which is equivalent to $c_\mu < 4$. Note that the stability condition does not put any constraint on the phase of μ .

Let $r(t) = V''(t; \hat{\mu}(t-1))$, $z_y(t) = \partial y(t; \hat{\mu}(t-1))/\partial \mu$ and $\mathbf{z}_\alpha(t) = \partial \hat{\alpha}(t+1|t; \hat{\mu}(t-1))/\partial \mu$. Then SONIC algorithm can be summarized as follows

$$\begin{aligned}z_y(t) &= -c_\mu \mathbf{f}^\top(t) \hat{\mathbf{M}}^{-1}(t-1) \mathbf{z}_\alpha(t-1) \\ \mathbf{z}_\alpha(t) &= \mathbf{z}_\alpha(t-1) + \hat{\mathbf{M}}(t-1) \mathbf{f}(t) z_y(t) + \mathbf{H} \mathbf{f}(t) y(t) \\ r(t) &= \rho r(t-1) + |z_y(t)|^2 \\ \hat{\mu}(t) &= \hat{\mu}(t-1) - \frac{z_y^*(t) y(t)}{r(t)} \\ \hat{\mathbf{M}}(t) &= \begin{bmatrix} \text{Re}\{\hat{\mu}(t)\} & -\text{Im}\{\hat{\mu}(t)\} \\ \text{Im}\{\hat{\mu}(t)\} & \text{Re}\{\hat{\mu}(t)\} \end{bmatrix} \\ \hat{\alpha}(t+1|t) &= \hat{\alpha}(t|t-1) + \hat{\mathbf{M}}(t) \mathbf{f}(t) y(t) \\ u(t) &= -\hat{\alpha}^\top(t+1|t) \mathbf{K}_n^{-1} \mathbf{f}(t+1)\end{aligned}\quad (35)$$

Remark: The control rule (17) was based on an implicit assumption that $\mathbf{K}_n = \mathbf{K}_0$, i.e., that $\beta = 1$. A similar technique, called coefficient fixing, is often used to “robustify” self-tuning minimum-variance regulators [16], [17]. In both cases, under certain conditions, the modeling biases are automatically compensated when estimation is carried in a closed loop. Substitution $\beta = c_\mu/\mu$ can be considered a modified version of the coefficient fixing technique. In Section VI we will show that even though the assumed value of β usually differs from the true one, the values of $\hat{\mu}(t)$, computed using the algorithm (35), converge in mean to the optimal value μ_{opt} . One can show that, similarly as in the case of complex-valued systems, the substitution $\beta = 1$ (which might look as a more “natural” choice) does not allow one to compensate phase modeling errors greater than $\pi/2$ – see [7] for more details.

V. MEAN CONVERGENCE ANALYSIS

Consider the simplified version of the algorithm (35), obtained by setting

$$\hat{\mu}(t) = \hat{\mu}(t-1) - c_r z_y^*(t) y(t) \quad (36)$$

where c_r denotes a small positive constant. The introduced modification – replacement of the time-varying gain $1/r(t)$, in the fourth recursion of (35), with a constant gain c_r – turns the RPE-based control algorithm into a gradient-based algorithm, which is easier to analyze.

According to [11], [18], for sufficiently small values of c_r , the estimates $\hat{\mu}(t)$ wander around μ_0 – the stable “equilibrium point” of the ordinary differential equation (ODE) associated with the algorithm (36). Such stable equilibrium point must obey the following conditions:⁴

$$g(\mu_0) = 0, \quad \text{Re}[g'(\mu_0)] > 0 \quad (37)$$

where

$$g(\mu) = \text{E}[y(t; \mu) z_y^*(t; \mu)], \quad g'(\mu) = \partial g(\mu) / \partial \mu$$

and $\{y(t; \mu)\}$, $\{z_y(t; \mu)\}$ are stationary processes that “settle down” in the closed-loop system for a constant value of μ : $\hat{\mu}(t) \equiv \mu \in \Omega_s$.

In Appendix we prove the following

Proposition 1: Under assumptions (A1)–(A3) it holds that

$$\mu_0 = \mu_{\text{opt}}. \quad (38)$$

Then, under some additional regularity conditions, stated in [18], one arrives at the following result (which is a specialisation of Theorem 3 in [18]):

Proposition 2: For c_r sufficiently small and $\epsilon > 0$, there exists a constant $D(c_r)$ such that

$$\limsup_{t \rightarrow \infty} \text{P}\{|\hat{\mu}(t) - \mu_0| > \epsilon\} \leq D(c_r)$$

where $D(c_r)$ tends to zero as c_r tends to zero.

The last two results mean that the proposed adaptive regulator converges (locally) in mean to the optimal regulator, i.e., the initial modeling errors are compensated by feedback.

Careful examination of the derivation presented in the Appendix leads to the conclusion that both propositions remain valid for the original (unmodified) RPE algorithm (35).

Comments: 1) It should be stressed that Proposition 2 is *not* a stochastic stability result. This is because the ODE-based analysis does not cover phenomena called large deviations or rare events. In fact, one of important technical assumptions made in [18] says that $\hat{\mu}(t)$ should at all times remain in Ω_0 – the domain of attraction of μ_0 (which, in general, is a subset of Ω_s , centered around μ_0).⁵ Since the difference $\hat{\mu}(t) - \mu_0$ cannot be claimed uniform along the whole trajectory, corresponding to a given realization of noise, the estimator $\hat{\mu}(t)$ may eventually escape from Ω_0 . According to Proposition 2 the probability of such an event goes to zero as c_r becomes small. Outside the domain Ω_0 the Markov chain, representing the “state” of the analyzed algorithm, is no longer recurrent but transient, and in general explosive.

⁴Under the assumption that $g^\dagger(\mu_0) = 0$, $g^\dagger(\mu) = \partial g(\mu) / \partial \mu^*$, which can be easily verified in the case considered – see Appendix B

⁵The ODE associated with (35) has the form: $\dot{\mu} = g(\mu)$. The domain of attraction Ω_0 is the set of initial conditions which guarantee that solution of this equation converges to μ_0 .

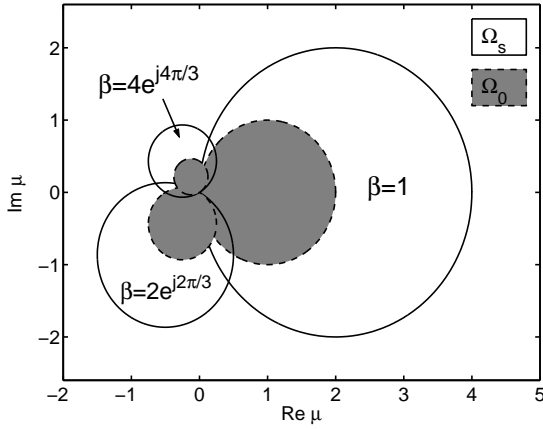


Fig. 3. Stability (Ω_s) and attraction (Ω_0) domains for different values of modeling errors ($\beta = 1$ corresponds to exact knowledge of the plant's gain).

Therefore, some extra precautions are needed to guarantee system stability – see next comment.

2) We have a rich simulation evidence suggesting that the proposed regulator has the so-called self-stabilization property. This means that the algorithm leaves the explosive zone of its own accord. The self-stabilization mechanism is typical of adaptive minimum-variance regulators: when instability occurs, it causes rapid growth of the output signal, which in turn speeds up convergence of $\hat{\mu}$ to a new stabilizing value. In this way, after a short burst observed at the system output, the closed-loop stability is regained – see Section VII-B for more comments on this issue. Unfortunately, no mathematical analysis of this phenomenon can be presented at the moment.

3) To avoid bursting behavior in the initial phase of convergence, one should pick $\hat{\mu}(0) \in \Omega_0$. However, since the domain of attraction Ω_0 depends on the modeling error β (which is unknown), this may be difficult to accomplish. Vaguely speaking, the domain Ω_0 “shrinks” as the magnitude and phase components of the modeling error grow – see Fig. 3. Therefore it is certainly beneficial to have a good prior knowledge of the true plant response \mathbf{K}_0 at the initial stage of adaptation. Our practical recommendation is to set $\hat{\mu}(0)$ to a small real number, e.g. in all numerical experiments described in Section VII we have adopted $\hat{\mu}(0) = 0.02$.

VI. SAFEGUARDS

Following [7] we will propose modifications increasing robustness of the proposed disturbance rejection scheme.

First, to avoid erratic behavior of the algorithm during startup/transient periods, it is advisable to set the maximum allowable values for $|\hat{\mu}(t)|$, $|\hat{\mu}(t) - \hat{\mu}(t-1)|$ and $r(t)$, further denoted by μ_{\max} , $\Delta\mu_{\max}$ and r_{\max} , respectively. These are typical “safety valves” used in adaptive control.

Second, instead of a constant forgetting factor ρ , one can use in (35) a time-varying factor dependent on the current value of μ

$$\rho(t) = 1 - c_\rho |\hat{\mu}(t-1)|$$

where $0 < c_\rho \ll 1$. This ensures that $1 - \rho$ will be at all times much smaller than $\hat{\mu}$, which is required for the overall system to work correctly [8].

Denote by $\text{sat}(x, a)$, $x \in \mathbb{C}$, $a \in \mathbb{R}_+$, a complex-valued saturation function

$$\text{sat}(x, a) = \begin{cases} x, & \text{if } |x| \leq a \\ a \frac{x}{|x|}, & \text{if } |x| > a \end{cases}.$$

Then the modified SONIC algorithm, that combines all “fixes” described above, can be summarized as follows

$$\begin{aligned} z_y(t) &= -c_\mu \mathbf{f}^\top(t) \hat{\mathbf{M}}^{-1}(t-1) \mathbf{z}_\alpha(t-1) \\ \mathbf{z}_\alpha(t) &= \mathbf{z}_\alpha(t-1) + \hat{\mathbf{M}}(t-1) \mathbf{f}(t) z_y(t) + \mathbf{H} \mathbf{f}(t) y(t) \\ \rho(t) &= 1 - c_\rho |\hat{\mu}(t-1)| \\ \tilde{r}(t) &= \rho(t) r(t-1) + |z_y(t)|^2 \\ r(t) &= \min(\tilde{r}(t), r_{\max}) \\ \Delta\mu(t) &= \text{sat}(z_y^*(t) y(t) / r(t), \Delta\mu_{\max}) \\ \tilde{\mu}(t) &= \hat{\mu}(t-1) - \Delta\mu(t) \\ \hat{\mu}(t) &= \text{sat}(\tilde{\mu}(t), \mu_{\max}) \\ \hat{\mathbf{M}}(t) &= \begin{bmatrix} \text{Re}\{\hat{\mu}(t)\} & -\text{Im}\{\hat{\mu}(t)\} \\ \text{Im}\{\hat{\mu}(t)\} & \text{Re}\{\hat{\mu}(t)\} \end{bmatrix} \\ \hat{\boldsymbol{\alpha}}(t+1|t) &= \hat{\boldsymbol{\alpha}}(t|t-1) + \hat{\mathbf{M}}(t) \mathbf{f}(t) y(t) \\ u(t) &= -\hat{\boldsymbol{\alpha}}^\top(t+1|t) \mathbf{K}_n^{-1} \mathbf{f}(t+1) \end{aligned} \quad (39)$$

VII. EXTENSIONS

We will describe two extensions of the proposed control scheme: to systems with multiharmonic disturbances and to systems with an extra transport delay.

A. Multiharmonic disturbances

Sinusoidal disturbances that occur in vibrating systems often consist of the fundamental (with frequency ω_0) and several harmonics (with frequencies $2\omega_0$, $3\omega_0$ etc.). Suppose that m such components, with slowly-varying amplitudes, are present:

$$d(t) = \sum_{i=1}^m d_i(t)$$

$$\begin{aligned} d_i(t) &= \boldsymbol{\alpha}_i^\top(t) \mathbf{f}_i(t), & \mathbf{f}_i(t) &= [\sin \omega_0 i t, \cos \omega_0 i t]^\top \\ \boldsymbol{\alpha}_i(t) &= [a_{1i}(t), a_{2i}(t)]^\top, & \boldsymbol{\alpha}_i(t) &= \boldsymbol{\alpha}_i(t-1) + \mathbf{w}_i(t) \end{aligned}$$

where $\{\mathbf{w}_i(t)\}$, $i = 1, \dots, m$, are mutually independent white noise sequences with covariance matrices $\sigma_1^2 \mathbf{I}, \dots, \sigma_m^2 \mathbf{I}$, respectively.

Rejection of a multiharmonic disturbance can be achieved by employing a parallel estimation algorithm made up of m subalgorithms, of the form described in the previous section, designed to eliminate different components of $d(t)$

$$\begin{aligned} \hat{\boldsymbol{\alpha}}_i(t+1|t) &= \hat{\boldsymbol{\alpha}}_i(t|t-1) + \mathbf{M}_i \mathbf{f}_i(t) y(t) \\ i &= 1, \dots, m \\ u(t) &= -\sum_{i=1}^m \hat{\boldsymbol{\alpha}}_i^\top(t+1|t) \mathbf{K}_i^{-1} \mathbf{f}_i(t+1) \end{aligned} \quad (40)$$

where $\mathbf{K}_1, \mathbf{K}_2, \dots, \mathbf{K}_m$ denote the nominal plant gain matrices (evaluated at the frequencies $\omega_0, 2\omega_0, \dots, m\omega_0$) and

$$\mathbf{M}_i = \begin{bmatrix} \text{Re}\{\mu_i\} & -\text{Im}\{\mu_i\} \\ \text{Im}\{\mu_i\} & \text{Re}\{\mu_i\} \end{bmatrix}, \quad i = 1, \dots, m$$

are the adaptation gain matrices – see [7] for further justification of the structure of (40). The estimates of the complex-valued adaptation gain coefficients μ_i can be computed recursively (independently of one another) using the algorithm designed for the single frequency case.

B. Additional transport delay

Suppose that the plant is governed by

$$y(t) = K_0(q^{-1})u(t - \tau) + d(t) + v(t)$$

where τ denotes transport delay. So far we have considered the unit delay case. Some modifications are needed to cope with $\tau > 1$.

First, the control rule (17) should be replaced with

$$u(t) = -\hat{\alpha}^T(t + \tau|t)\mathbf{K}_n^{-1}\mathbf{f}(t + \tau) \quad (41)$$

where

$$\hat{\alpha}(t + \tau|t) = \hat{\alpha}(t + \tau - 1|t - 1) + \mathbf{M}\mathbf{f}(t)y(t). \quad (42)$$

Second, since in the case considered

$$y(t) \cong d(t) - \mathbf{f}^T(t)\mathbf{B}^T\hat{\alpha}(t|t - \tau) + v(t)$$

one should replace (31) with

$$\begin{aligned} \frac{\partial y(t)}{\partial \mu} &= -\mathbf{f}^T(t)\mathbf{B}^T \frac{\partial \hat{\alpha}(t|t - \tau)}{\partial \mu} \\ \frac{\partial \hat{\alpha}(t + \tau|t)}{\partial \mu} &= \frac{\partial \hat{\alpha}(t + \tau - 1|t - 1)}{\partial \mu} + \mathbf{M}\mathbf{f}(t) \frac{\partial y(t)}{\partial \mu} \\ &\quad + \frac{\partial \mathbf{M}}{\partial \mu} \mathbf{f}(t)y(t). \end{aligned} \quad (43)$$

Finally, after incorporating (32) and (33), one arrives at

$$\begin{aligned} \frac{\partial y(t)}{\partial \mu} &= -c_\mu \mathbf{f}^T(t)\mathbf{M}^{-1} \frac{\partial \hat{\alpha}(t|t - \tau)}{\partial \mu} \\ \frac{\partial \hat{\alpha}(t + \tau|t)}{\partial \mu} &= \frac{\partial \hat{\alpha}(t + \tau - 1|t - 1)}{\partial \mu} + \mathbf{M}\mathbf{f}(t) \frac{\partial y(t)}{\partial \mu} \\ &\quad + \mathbf{H}\mathbf{f}(t)y(t). \end{aligned} \quad (44)$$

When incorporating (44) into the adaptive control algorithm analogous to (35) or (39), one should replace \mathbf{M}^{-1} , appearing in the first recursion of (44), with $\widehat{\mathbf{M}}^{-1}(t - \tau)$, and replace \mathbf{M} with $\widehat{\mathbf{M}}(t - 1)$ in the second recursion.

VIII. SIMULATION RESULTS

To enable comparison with the results obtained for complex-valued input/output signals, all simulation experiments presented below are identical with those described in [7].

A. Steady-state performance

The purpose of this experiment was to examine the steady-state error compensation capabilities of the algorithm (35). None of the proposed safety jacketing measures was applied. The only user-dependent tuning “knob” ρ was set to 0.9999. Simulations were carried for the Guo & Bodson plant (30) with the following measurement noise and sinusoidal disturbance settings: $\sigma_v = 0.1$, $\sigma_w = 0.001/\sqrt{2}$, $c_\mu = 0.02$, $\omega_0 = 0.1$, $\alpha(0) = [0.5, 0.5]^T$. In the absence of modeling errors the

optimal value of μ is under such conditions equal to $\mu_{\text{opt}} = h_\infty = 0.01$.

Tables I and II show the mean-squared output errors (Table I) and mean-squared cancellation errors (Table II) observed for different values of β (12 selections, characterized in terms of magnitude and phase errors). All numbers were obtained by means of combined ensemble (100 realizations of $\{v(t)\}$ and $\{w(t)\}$) and time ($t \in [10001, 40000]$) averaging, after the algorithm has reached its steady-state behavior.

$\arg\beta [^\circ]$	$ \beta = 0.25$	$ \beta = 1$	$ \beta = 4$
0	1.0118	1.0119	1.0120
60	1.0118	1.0119	1.0120
120	1.0118	1.0119	1.0120
180	1.0118	1.0119	1.0120

TABLE I
STEADY-STATE MEAN-SQUARED OUTPUT-ERROR $E_\infty[y^2(t)] \cdot 10^{-2}$ MEASURED FOR DIFFERENT MAGNITUDE AND PHASE MODELING ERRORS. THE THEORETICAL LOWER ERROR BOUND IS IN THIS CASE EQUAL TO $1.01 \cdot 10^{-2}$

$\arg\beta [^\circ]$	$ \beta = 0.25$	$ \beta = 1$	$ \beta = 4$
0	1.0227	1.0389	1.0551
60	1.0228	1.0390	1.0553
120	1.0228	1.0389	1.0554
180	1.0228	1.0389	1.0553

TABLE II
STEADY-STATE MEAN-SQUARED CANCELLATION ERROR $E_\infty[\langle c^2(t) \rangle_\infty] \cdot 10^{-4}$ MEASURED FOR DIFFERENT MAGNITUDE AND PHASE ERRORS. THE THEORETICAL LOWER BOUND IS IN THIS CASE EQUAL TO $1.0025 \cdot 10^{-4}$

Note that the proposed control scheme is insensitive to phase errors and almost insensitive to magnitude errors. In all cases considered the mean-squared output errors are by less than 0.2% larger than the minimum error achievable when μ is set to its optimal value $\mu_{\text{opt}} = h_\infty/\beta$ and not estimated. The analogous degradation for the mean-squared cancellation errors does not exceed 6%. This means that the proposed disturbance rejection scheme is doing a remarkably good job in compensating modeling errors and optimizing the closed-loop system performance.

B. Transient performance

The objective of this experiment was to demonstrate the ability of the proposed algorithm to cope with sudden plant changes. The plant was changed three times during each simulation run – see Table III. The corresponding transfer functions are listed below:

$$\begin{aligned} K_1(z) &= \frac{0.0952}{1 - 0.9048z^{-1}} \\ K_2(z) &= \frac{0.0238}{1 - 0.9762z^{-1}} \\ K_3(z) &= \frac{0.2}{1 - 0.8z^{-1}} \\ K_4(z) &= \frac{-0.1 + 0.14z^{-1}}{1 - 1.8391z^{-1} + 0.8649z^{-2}}. \end{aligned}$$

At all times the nominal plant gain was kept at the constant level $\mathbf{K}_n = \mathbf{I}$. While the first two changes (from $K_1(z)$ to $K_2(z)$ at instant $t = 15000$ and from $K_2(z)$ to $K_3(z)$ at instant $t = 30000$) were confined to plant parameters, the last one was more substantial: at instant $t = 45000$ the first-order inertial system $K_3(z)$ with a single real pole was switched to the second-order nonminimum phase system $K_4(z)$ with a pair of complex poles. Since the phase shift introduced by $K_4(z)$ at frequency ω_0 differs from the analogous shift of $K_3(z)$ by more than $\pi/2$ [which means that the stabilizing gain $\hat{\mu}$ for $K_3(z)$ does not stabilize $K_4(z)$], the last change causes temporal instability of the closed-loop system, making the task of disturbance rejection even harder.

Time interval	Plant	$ \beta $	$\arg\beta[^\circ]$
$0 < t < 15000$	$K_1(z)$	0.708	-42.2
$15000 \leq t < 30000$	$K_2(z)$	0.234	-73.6
$30000 \leq t < 45000$	$K_3(z)$	0.913	-21.4
$45000 \leq t \leq 60000$	$K_4(z)$	1.960	126.8

TABLE III
PLANT SWITCHING SCHEDULE IN THE TRANSIENT BEHAVIOR EXPERIMENT AND THE CORRESPONDING MODELING ERRORS.

Fig. 3 shows the results of a typical simulation run obtained for the algorithm (39) with the following settings: $c_p = 0.05$, $c_\mu = 0.005$, $\mu_{\max} = 0.05$, $\Delta\mu_{\max}(t) = \hat{\mu}(t-1)/50$, $r_{\max} = 2000$. The “cold start” procedure was used, i.e., the adaptation process was started from scratch at instant $t = 1$ using the following initial conditions: $r(0) = 100$, $z_\alpha(0) = 0$, $\hat{\mu}(0) = 0.02$. The algorithm dealt favorably with both the initial convergence problem and with abrupt plant changes. When the experiment was started or when a change to the plant dynamics occurred, the magnitude of the adaptation gain $\hat{\mu}(t)$ temporarily increased to quickly compensate large initial modeling errors; later on it gradually decayed to settle down around its optimal steady-state value. Note very quick response to phase errors and (usually) much slower response to magnitude errors – the effect caused by diverse sensitivity of system output to two types of modeling errors.

Simulation experiments confirm that the proposed control scheme has the self-stabilization property. Note how stability, lost at instant $t = 45000$, is quickly regained after a short burst observed at the system output. We have found out experimentally, that this burst can be reduced, both in size and duration, if a very simple stability safeguard is added to (39), namely if the sign of the adaptation gain is changed when the magnitude of the output signal exceeds its maximum allowable value

$$\hat{\mu}(t) = -\hat{\mu}(t-1) \quad \text{if } |y(t)| > y_{\max}. \quad (45)$$

When polarity of $\hat{\mu}$ is changed, the sensitivity derivative $z_\alpha(t)$ should be set to zero. Additionally, to avoid multiple sign changes, after each intervention the stability enforcement mechanism (45) should be temporarily switched off. Selection of y_{\max} should be done with caution and usually requires some prior knowledge about the plant and/or disturbance – too small values of y_{\max} may trigger the stability rescue mechanism

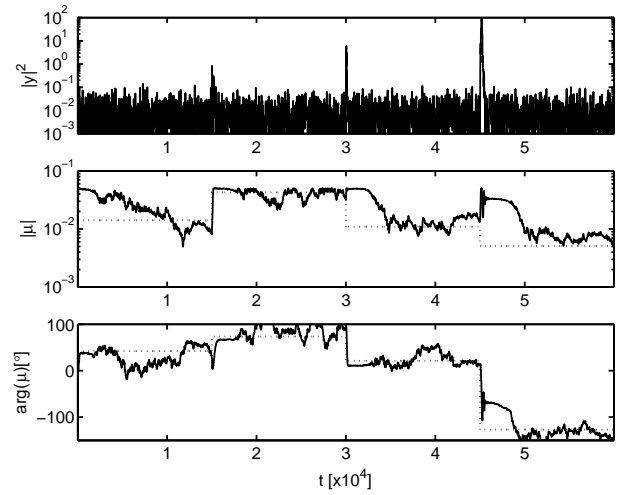


Fig. 4. Transient behavior of the disturbance rejection algorithm (results of a typical simulation run). Solid lines – estimated values, dotted lines – optimal steady-state values.

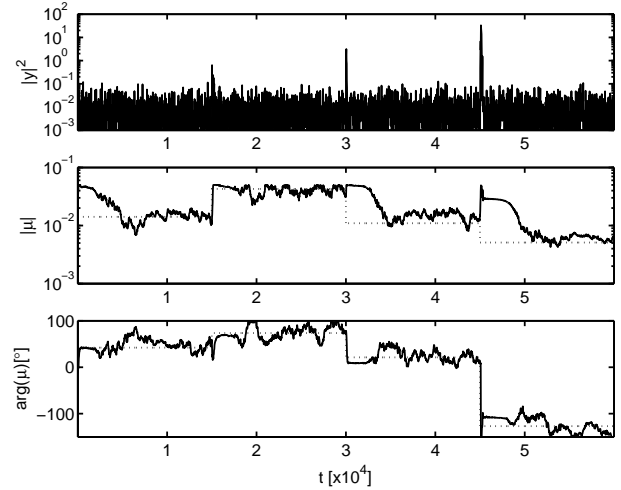


Fig. 5. Transient behavior of the disturbance rejection algorithm equipped with a stability safeguard (results of a typical simulation run). Solid lines – estimated values, dotted lines – optimal steady-state values.

when such intervention is not really needed, e.g. when large values of $y(t)$ are *not* caused by system instability.

Fig. 5 (illustrating typical behavior) and Fig. 6 (illustrating mean behavior) show results obtained when the stability enforcement mechanism, described above, was applied with $y_{\max} = 5$. After a sign change this mechanism was blocked until $\bar{y}(t) = \max\{|y(t-i+1)|, i = 1, \dots, [T_0]\}$ dropped below 1. Note that the burst at the system output at instant $t = 45000$ was reduced to an acceptable level.

Three close-up views of the plots shown in Fig. 6 are presented in Fig. 7. In all cases the mean transient response is shorter than 500 samples, i.e., it lasts for less than 8 periods of the disturbance ($T_0 = 2\pi/\omega_0 \cong 63$). For less significant plant changes the length of the transient period is usually much shorter, often taking the values smaller than T_0 .

C. Multiharmonic disturbance

In our third experiment the output of the Guo & Bodson plant was corrupted with a sinusoidal signal consisting of the

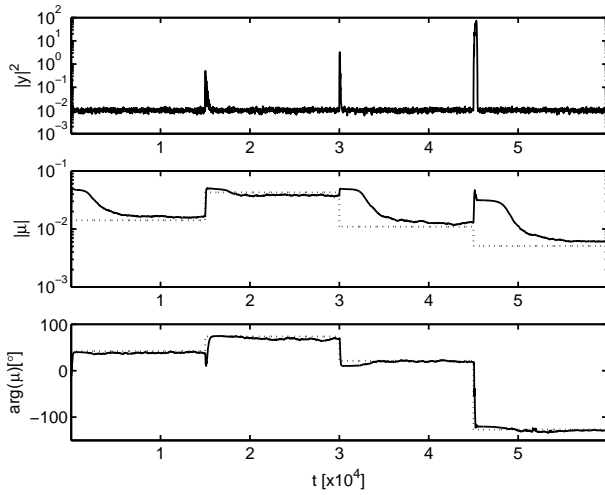


Fig. 6. Mean transient behavior of the disturbance rejection algorithm (average of 100 simulation runs). Solid lines – ensemble averages of the estimated values, dotted lines – optimal steady-state values.

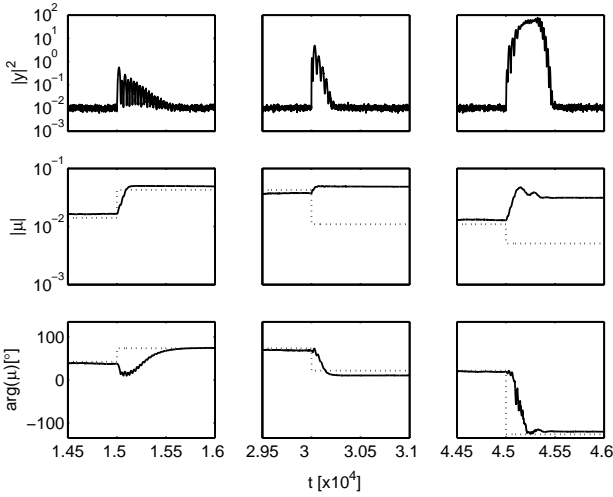


Fig. 7. Mean transient behavior of the disturbance rejection algorithm (average of 100 simulation runs) – close-up views of three plant switching areas. Solid lines – ensemble averages of the estimated values, dotted lines – optimal steady-state values.

first and third harmonics

$$d(t) = d_1(t) + d_3(t)$$

$$d_1(t) = \alpha_1^T(t) \mathbf{f}_1(t), \quad d_3(t) = \alpha_3^T(t) \mathbf{f}_3(t)$$

$$\mathbf{f}_1(t) = [\sin \omega_0 t, \cos \omega_0 t]^T, \quad \mathbf{f}_3(t) = [\sin 3\omega_0 t, \cos 3\omega_0 t]^T$$

where $\omega_0 = 0.1$ and $\alpha_1(t)$, $\alpha_3(t)$ changed according to the random-walk model: $\sigma_1 = \sigma_3 = 0.001/\sqrt{2}$, $\alpha_1(0) = [1, 1]^T$, $\alpha_3(0) = [0.5, 0.5]^T$. The measurement noise variance was equal to $\sigma_v^2 = 0.01$. The decentralized adaptive controller (40) was applied, combining two algorithms of the form (39) with identical settings: $c_{\rho,1} = c_{\rho,3} = 0.05$, $c_{\mu,1} = c_{\mu,3} = 0.005$, $r_{\max,1} = r_{\max,3} = 1600$, $\Delta\mu_{\max,1}(t) = \hat{\mu}_1(t-1)/50$, $\Delta\mu_{\max,3}(t) = \hat{\mu}_3(t-1)/50$, $\mu_{\max,1} = \mu_{\max,3} = 0.05$. The initial conditions were set to $\hat{\alpha}_1(0) = \hat{\alpha}_3(0) = [0, 0]^T$ and $\hat{\mu}_1(0) = \hat{\mu}_3(0) = 0.02$. Finally, the nominal plant gain matrices were set to $\mathbf{K}_1 = \mathbf{K}_3 = \mathbf{I}$, which resulted in the

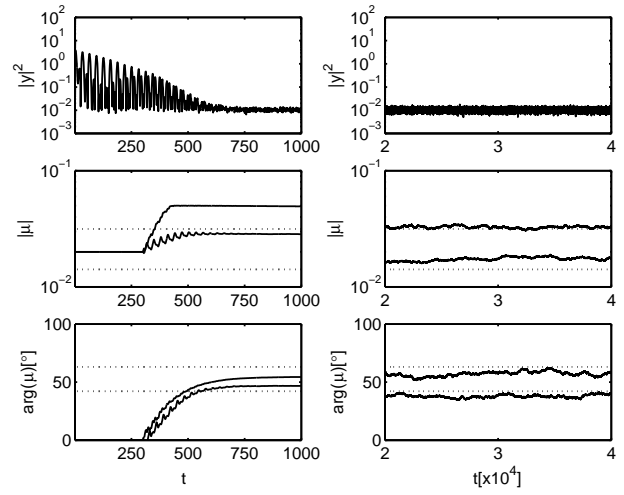


Fig. 8. Rejection of a multiharmonic disturbance (average of 100 simulation runs). Solid lines – ensemble averages of estimated values, dotted lines – optimal steady-state values.

following modeling errors: $|\beta_1| = 0.708$, $\arg\beta_1 = 42.2^\circ$, $|\beta_3| = 0.318$, $\arg\beta_3 = 74.6^\circ$.

This time a somewhat more cautious initialization scheme was used. During the first 300 time-steps the quantities $z_{\alpha,1}(t)$, $r_1(t)$ and $z_{\alpha,3}(t)$, $r_3(t)$ were evaluated but the adaptation gains $\hat{\mu}_1(t)$, $\hat{\mu}_3(t)$ were kept at their starting values $\hat{\mu}_1(0)$, $\hat{\mu}_3(0)$ and not updated. Then, at the instant $t = 301$, the adaptation lock was released.

Fig. 8 shows the results of a typical simulation run. Similarly as in the previous experiment, at the beginning of each transient phase the magnitudes of adaptation gains $\hat{\mu}_1(t)$ and $\hat{\mu}_3(t)$ took large values. Later on they slowly approached their steady-state optimal levels. In contrast with this, response to phase errors was pretty quick.

D. Additional transport delay

The transient behavior experiment, reported in Section VIII-B, was repeated with an extra transport delay, equal to 5 sampling intervals ($\tau = 6$), added to all plants. The algorithm (41)–(44) was used, equipped with the safety and stability enforcement mechanisms described earlier. The adaptation was started at instant $t = 1$ in an analogous way as described in Section VIII-B. The assumed nominal gain \mathbf{K}_n was equal to \mathbf{I} .

Fig. 9 shows the results of a typical simulation run. Note that these results are comparable with those presented in Fig. 5 for a plant with unit delay (in both cases the same realizations of $\{\mathbf{w}(t)\}$ and $\{v(t)\}$ were used).

IX. CONCLUSION

The problem of elimination of a sinusoidal disturbance of known frequency, acting at the output of an unknown linear stable plant was considered. The proposed solution is based on coefficient fixing – the technique originally developed for the purpose of adaptive minimum-variance control – combined with automatic adaptation gain adjustment. Both theoretical analysis and computer simulations confirm that when the

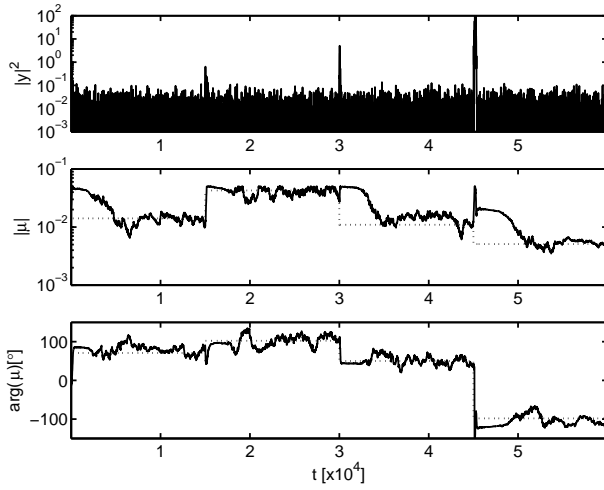


Fig. 9. Transient behavior of the disturbance rejection algorithm for a plant with extra transport delay (results of a typical simulation run). Solid lines – estimated values, dotted lines – optimal steady-state values.

amplitudes of the disturbance evolve according to the random-walk model, the resulting regulator converges (locally) in mean to the optimal regulator. To the best of our knowledge it is the first adaptive vibration controller with self-optimization capability.

REFERENCES

- [1] M. Bodson and S. Douglas, “Adaptive algorithms for the rejection of sinusoidal disturbances with unknown frequency,” *Automatica*, vol. 33, pp. 2213–2221, Dec. 1997.
- [2] M. Bodson, “Performance of an adaptive algorithm of sinusoidal disturbance rejection in high noise,” *Automatica*, vol. 37, pp. 1133–1140, July 2001.
- [3] B. Wu and M. Bodson, “Multi-channel active noise control for periodic sources - indirect approach,” *Automatica*, vol. 40, pp. 203–212, Feb. 2004.
- [4] X. Guo and M. Bodson, “Adaptive rejection of multiple sinusoids of unknown frequency,” in *Proc. European Control Conference*, Kos, Greece, 2007, pp. 121–128.
- [5] I.D. Landau, A. Constantinescu, and D. Rey, “Adaptive narrow band disturbance rejection applied to an active suspension - an internal model principle approach,” *Automatica*, vol. 41, pp. 563–574, April 2005.
- [6] I.D. Landau and D. Patrascu, “Rejection of unknown multiple narrow band disturbances - a direct adaptive control approach,” in *Proc. European Control Conference*, Kos, Greece, 2007, pp. 135–141.
- [7] M. Niedźwiecki and M. Meller, “A study in vibration control: the unknown plant - known frequency case,” Gdańsk University of Technology, Tech. Rep. ETI-1/2008, 2008. [Online]. Available: <http://www.eti.pg.gda.pl/katedry/ksa/pracownicy/Maciej.Niedzwiecki>
- [8] —, “Tracking analysis of an adaptive vibration controller,” in *Proc. 47th CDC*, Cancun, Mexico, 2008.
- [9] F. Lewis, *Optimal Estimation*. New York: Wiley, 1986.
- [10] E.-W. Bai, L.-C. Fu, and S. Sastry, “Averaging analysis for discrete time and sampled data adaptive systems,” *IEEE Trans. Circuits Syst.*, vol. 35, pp. 137–148, Feb. 1988.
- [11] A. Benveniste and G. Ruget, “A measure of the tracking capability of recursive stochastic algorithms with constant gains,” *IEEE Trans. Autom. Control*, vol. 25, pp. 788–794, June 1982.
- [12] H. van Trees and E. K.L. Bell, Eds., *Bayesian Bounds for Parameter Estimation and Nonlinear Filtering/Tracking*. New York: Wiley, 2007.
- [13] M. Niedźwiecki, *Identification of Time-varying Processes*. New York: Wiley, 2000.
- [14] T. Söderström and P. Stoica, *System Identification*. Englewood Cliffs NJ: Prentice Hall, 1988.
- [15] S. Haykin, *Adaptive Filter Theory*. Englewood Cliffs NJ: Prentice Hall, 1996.
- [16] K. Åström, U. Borisson, L. Ljung, and B. Wittenmark, “Theory and applications of self-tuning regulators,” *Automatica*, vol. 13, pp. 457–476, Sept. 1977.
- [17] M. Niedźwiecki, “Steady-state and parameter tracking properties of self-tuning minimum variance regulators,” *Automatica*, vol. 25, pp. 597–602, July 1989.
- [18] A. Benveniste, M. Métivier, and P. Priouret, *Adaptive Algorithms and Stochastic Approximations*. Springer-Verlag, 1990.

APPENDIX

PROOF OF PROPOSITION 1

A. Equilibrium point

First, we will derive the closed-form expression for $g(\mu) = E[y(t)z_y^*(t)]$ (for the sake of brevity dependence of $y(t)$, $z_y(t)$, $\hat{\alpha}(t)$ etc. on μ will be temporarily dropped). Observe that $y(t) = \Delta\hat{\alpha}^T(t)\mathbf{f}(t) + v(t)$ and $z_y(t) = -c_\mu\mathbf{f}^T(t)\mathbf{M}^{-1}\mathbf{z}_\alpha(t-1)$ which leads to

$$E[y(t)z_y^*(t)] = -c_\mu E[\Delta\hat{\alpha}^T(t)\mathbf{f}(t)\mathbf{f}^T(t)\mathbf{M}^{-1}\mathbf{z}_\alpha^*(t-1)] - c_\mu E[v(t)\mathbf{f}^T(t)\mathbf{M}^{-1}\mathbf{z}_\alpha^*(t-1)].$$

Note that the second term on the right-hand side of the last equation is zero due to orthogonality of $v(t)$ and $\mathbf{z}_\alpha^*(t-1)$. Applying averaging to the first term, one arrives at [cf. (12)]

$$E[y(t)z_y^*(t)] \cong -\frac{c_\mu}{2} E[\Delta\hat{\alpha}^T(t)\mathbf{M}^{-1}\mathbf{z}_\alpha^*(t-1)].$$

Using the relationships

$$\begin{aligned} \Delta\hat{\alpha}^T(t) &= \Delta\hat{\alpha}^T(t-1)[\mathbf{I} - \mathbf{f}(t-1)\mathbf{f}^T(t-1)\mathbf{M}^T\mathbf{B}] \\ &\quad - \mathbf{f}^T(t-1)\mathbf{M}^T\mathbf{B}v(t-1) + \mathbf{w}^T(t) \\ \mathbf{z}_\alpha^*(t-1) &= [\mathbf{I} - c_\mu\mathbf{M}\mathbf{f}(t-1)\mathbf{f}^T(t-1)\mathbf{M}^{-1}]\mathbf{z}_\alpha^*(t-2) \\ &\quad + \mathbf{H}^*\mathbf{f}(t-1)\mathbf{f}^T(t-1)\Delta\hat{\alpha}(t-1) \\ &\quad + \mathbf{H}^*\mathbf{f}(t-1)v(t-1) \end{aligned}$$

and dropping all terms that are zero due to orthogonality, one obtains

$$J(t) = E\{\Delta\hat{\alpha}^T(t)\mathbf{M}^{-1}\mathbf{z}_\alpha^*(t-1)\} = J_1(t) + J_2(t) + J_3(t)$$

where

$$\begin{aligned} J_1(t) &= E\{\Delta\hat{\alpha}^T(t-1)\mathbf{A}_1(t)\mathbf{z}_\alpha^*(t-2)\} \\ J_2(t) &= E\{\Delta\hat{\alpha}^T(t-1)\mathbf{A}_2(t)\Delta\hat{\alpha}(t-1)\} \\ J_3(t) &= -E\{\mathbf{f}^T(t-1)\mathbf{M}^T\mathbf{B}\mathbf{M}^{-1}\mathbf{H}^*\mathbf{f}(t-1)v^2(t-1)\} \end{aligned}$$

and the time-varying matrices $\mathbf{A}_1(t)$, $\mathbf{A}_2(t)$ are as follows

$$\begin{aligned} \mathbf{A}_1(t) &= [\mathbf{I} - \mathbf{f}(t-1)\mathbf{f}^T(t-1)\mathbf{M}^T\mathbf{B}] \mathbf{M}^{-1} \\ &\quad \times [\mathbf{I} - c_\mu\mathbf{M}\mathbf{f}(t-1)\mathbf{f}^T(t-1)\mathbf{M}^{-1}] \\ \mathbf{A}_2(t) &= [\mathbf{I} - \mathbf{f}(t-1)\mathbf{f}^T(t-1)\mathbf{M}^T\mathbf{B}] \\ &\quad \times \mathbf{M}^{-1}\mathbf{H}^*\mathbf{f}(t-1)\mathbf{f}^T(t-1). \end{aligned}$$

One can check that $\mathbf{f}^T(t-1)\mathbf{M}^T\mathbf{B}\mathbf{f}(t-1) = \text{Re}\{\beta\mu\}$, which leads to

$$\mathbf{A}_1(t) = [\mathbf{I} - \mathbf{f}(t-1)\mathbf{f}^T(t-1)\mathbf{M}^T\mathbf{B} - c_\mu\mathbf{f}(t-1)\mathbf{f}^T(t-1) + c_\mu\text{Re}\{\beta\mu\}\mathbf{f}(t-1)\mathbf{f}^T(t-1)] \mathbf{M}^{-1}$$

and

$$\langle \mathbf{A}_1(t) \rangle_\infty = [1 - c_\mu/2 + c_\mu\text{Re}\{\beta\mu\}/2] \mathbf{M}^{-1} - \mathbf{M}^T\mathbf{B}\mathbf{M}^{-1}/2.$$

Hence

$$\begin{aligned} J_1(t) &\cong \mathbb{E}\{\Delta\hat{\alpha}^T(t-1) < \mathbf{A}_1(t) >_{\infty} \mathbf{z}_{\alpha}^*(t-2)\} \\ &= [1 - c_{\mu}/2 + c_{\mu}\text{Re}\{\beta\mu\}/2] J(t-1) \\ &\quad - \mathbb{E}\{\Delta\hat{\alpha}^T(t-1)\mathbf{M}^T\mathbf{B}\mathbf{M}^{-1}\mathbf{z}_{\alpha}^*(t-2)\}/2. \end{aligned}$$

To further simplify $J_1(t)$ note that for small values of c_{μ} it holds that (after averaging)

$$\mathbf{z}_{\alpha}(t) = (1 - c_{\mu}/2)\mathbf{z}_{\alpha}(t-1) + \mathbf{H}\mathbf{f}(t)y(t).$$

Since

$$\mathbf{H}\mathbf{f}(t) = \frac{1}{2} \begin{bmatrix} 1 & j \\ -j & 1 \end{bmatrix} \begin{bmatrix} \sin \omega_0 t \\ \cos \omega_0 t \end{bmatrix} = \frac{e^{-j\omega_0 t}}{2} \begin{bmatrix} j \\ 1 \end{bmatrix}$$

one arrives at

$$\mathbf{z}_{\alpha}(t) = [z_{\alpha 1}(t), z_{\alpha 1}(t)]^T, \quad z_{\alpha 1}(t) = jz_{\alpha 2}(t).$$

It is straightforward to check that under the constraint derived above it holds that

$$\mathbf{M}^{-1}\mathbf{z}_{\alpha}^*(t) = \frac{\mathbf{z}_{\alpha}^*(t)}{\mu^*}, \quad \mathbf{M}^T\mathbf{B}\mathbf{z}_{\alpha}^*(t) = \beta\mu\mathbf{z}_{\alpha}^*(t)$$

which leads to

$$\Delta\hat{\alpha}^T(t-1)\mathbf{M}^T\mathbf{B}\mathbf{M}^{-1}\mathbf{z}_{\alpha}^*(t-2) = \beta\mu J(t-1).$$

Combining this with the earlier result, one obtains

$$J_1(t) = [1 - c_{\mu}/2 + c_{\mu}\text{Re}\{\beta\mu\}/2 - \beta\mu/2]J(t-1).$$

To evaluate $J_2(t)$ note that

$$\begin{aligned} \mathbf{M}^{-1}\mathbf{H}^* &= \frac{1}{\mu^*}\mathbf{H}^* \\ \mathbf{f}^T(t-1)\mathbf{M}^T\mathbf{B}\mathbf{M}^{-1}\mathbf{H}^*\mathbf{f}(t-1) &= \frac{\beta\mu}{2\mu^*} \end{aligned}$$

which leads to

$$\begin{aligned} \mathbf{A}_2(t) &= \frac{1}{\mu^*} [\mathbf{H}^* - \beta\mu\mathbf{I}/2] \mathbf{f}(t-1)\mathbf{f}^T(t-1) \\ \langle \mathbf{A}_2(t) \rangle_{\infty} &= \frac{1}{2\mu^*}\mathbf{H}^* - \frac{\beta\mu}{4\mu^*}\mathbf{I}. \end{aligned}$$

Finally, exploiting the fact that $\Delta\hat{\alpha}^T(t-1)\mathbf{H}^*\Delta\hat{\alpha}(t-1) = \|\Delta\hat{\alpha}(t-1)\|^2/2$ and $\Delta\hat{\alpha}^T(t-1)\Delta\hat{\alpha}(t-1) = \|\Delta\hat{\alpha}(t-1)\|^2$, one arrives at

$$\begin{aligned} J_2(t) &\cong \mathbb{E}\{\Delta\hat{\alpha}^T(t-1) < \mathbf{A}_2(t) >_{\infty} \Delta\hat{\alpha}(t-1)\} \\ &= \frac{1 - \beta\mu}{4\mu^*} \mathbb{E}\{\|\Delta\hat{\alpha}(t-1)\|^2\}. \end{aligned}$$

Evaluation of the term $J_3(t)$ is relatively easy

$$J_3(t) = -\frac{\beta\mu}{2\mu^*}\sigma_v^2.$$

After combining all partial results derived so far, equation $J(t) = J_1(t) + J_2(t) + J_3(t)$ constitutes a recursive formula for evaluation of $J(t) = \mathbb{E}\{\Delta\hat{\alpha}^T(t)\mathbf{M}^{-1}\mathbf{z}_{\alpha}^*(t-1)\}$

$$\begin{aligned} J(t) &\cong [1 - c_{\mu}/2 + c_{\mu}\text{Re}\{\beta\mu\}/2 - \beta\mu/2] J(t-1) \\ &\quad + \frac{1 - \beta\mu}{4\mu^*} \mathbb{E}\{\|\Delta\hat{\alpha}(t-1)\|^2\} - \frac{\beta\mu}{2\mu^*}\sigma_v^2 \end{aligned}$$

the steady-state solution of which (under suitable stability conditions) can be obtained in the form

$$\begin{aligned} J(\infty) &= \mathbb{E}_{\infty}\{\Delta\hat{\alpha}^T(t)\mathbf{M}^{-1}\mathbf{z}_{\alpha}^*(t-1)\} \\ &\cong \frac{(1 - \beta\mu)\mathbb{E}_{\infty}\{\|\Delta\hat{\alpha}(t)\|^2\}/2 - \beta\mu\sigma_v^2}{\mu^*[c_{\mu} + \beta\mu - c_{\mu}\text{Re}\{\beta\mu\}]} = \frac{N(\mu)}{D(\mu)}. \end{aligned}$$

To determine the equilibrium point μ_0 we shall require that

$$g(\mu_0) = \mathbb{E}_{\infty}\{y(t; \mu_0)z_y^*(t; \mu_0)\} = -\frac{c_{\mu}}{2}J(\infty) = 0$$

which is equivalent to $N(\mu_0) = 0$. Using (26) the latter condition can be rewritten as

$$\frac{(1 - \beta\mu_0)[\xi + |\beta\mu_0|^2/2]}{\beta\mu_0[\text{Re}\{\beta\mu_0\} - |\beta\mu_0|^2/2]} = 1.$$

Since $\beta\mu_0$ must be a positive real number, one finally obtains

$$\beta\mu_0 = -\xi + \sqrt{\xi^2 + 2\xi}$$

which, according to (27), means that $\mu_0 = \mu_{\text{opt}}$.

B. Local stability

Since $N(\mu_0) = 0$, one obtains

$$g'(\mu_0) = -\frac{c_{\mu}}{2} \cdot \frac{N'(\mu_0)}{D(\mu_0)}.$$

Furthermore, since μ_0 minimizes $\mathbb{E}_{\infty}\{\|\Delta\hat{\alpha}(t; \mu)\|^2\}$, it holds that $\mathbb{E}'_{\infty}\{\|\Delta\hat{\alpha}(t; \mu_0)\|^2\} = 0$, where the derivative is taken with respect to μ . Combining these results, one arrives at

$$g'(\mu_0) = \frac{c_{\mu}\beta\mu_0[\mathbb{E}_{\infty}\{\|\Delta\hat{\alpha}(t; \mu_0)\|^2\}/2 + \sigma_v^2]}{2|\mu_0|^2[c_{\mu} + (1 - c_{\mu})\beta\mu_0]} > 0.$$

In an analogous way one can show that $g^{\dagger}(\mu_0) = -N^{\dagger}(\mu_0)/D(\mu_0) = 0$.



Maciej Niedźwiecki (M'08) was born in Poznań, Poland in 1953. He received the M.Sc. and Ph.D. degrees from the Gdańsk University of Technology, Gdańsk, Poland, and the Dr.Hab. (D.Sc.) degree from the Technical University of Warsaw, Warsaw, Poland, in 1977, 1981 and 1991, respectively.

He spent three years as a Research Fellow with the Department of Systems Engineering, Australian National University, 1986-1989. In 1990 - 1993 he served as a Vice Chairman of Technical Committee on Theory of the International Federation of Automatic Control (IFAC). He is the author of the book *Identification of Time-varying Processes* (Wiley, 2000).

He works as a Professor and Head of the Department of Automatic Control, Faculty of Electronics, Telecommunications and Computer Science, Gdańsk University of Technology. His main areas of research interests include system identification, signal processing and adaptive systems.



Michał Meller (S'08) received the M.Sc. degree in automatic control from Gdańsk University of Technology, Gdańsk, Poland, in 2007. Since 2007 he has been working in Telecommunications Research Institute S.A. Gdańsk Division, Department of Signal and Information Processing. He is also pursuing his Ph.D. in the the Department of Automatic Control, Faculty of Electronics, Telecommunications and Computer Science, Gdańsk University of Technology. His professional interests include signal processing and adaptive systems.